Colloids and Surfaces B: Biointerfaces 129 (2015) 183–190

Contents lists available at ScienceDirect

Colloids and Surfaces B: Biointerfaces

journal homepage: www.elsevier.com/locate/colsurfb

The antimicrobial peptide microcin J25 stabilizes the gel phase of bacterial model membranes

M.R. Rintoul, R.D. Morero, F.G. Dupuy*

Instituto Superior de Investigaciones Biológicas (INSIBIO), CONICET-UNT, and Instituto de Química Biológica "Dr. Bernabé Bloj", Facultad de Bioquímica, Química y Farmacia, UNT, Chacabuco 461, T4000ILI San Miguel de Tucumán, Argentina

ARTICLE INFO

Article history:
Received 19 November 2014
Received in revised form 19 March 2015
Accepted 20 March 2015
Available online 30 March 2015

Keywords:
Microcin J25
Bacterial membrane model systems
Ordered lipid phase stabilization

ABSTRACT

The bacterial membrane interaction of the antimicrobial peptide microcin J25 was studied with the probe-free techniques Langmuir monolayers and infrared spectroscopy. Membrane model systems composed by phosphatidylethanolamine:phosphatidylglycerol 7:3, which mimic the cytoplasmic membrane of Gram negative bacteria, were used in both monolayer and bilayer approaches. The peptide reduced the transition surface pressure of the expanded-to-condensed lipid monolayer states, as well as increased the gel-to-liquid crystalline transition temperature in bilayers, indicating a stabilization of membrane ordered state. In addition, a reduction of the surface pressure at which condensed domains appeared was observed upon mixed monolayers compression after microcin J25 adsorption. The results indicate a favorable interaction of microcin J25 with bacterial membrane model systems. Also, the effects on the ordered phases stabilization are discussed in terms of the biological effects observed in membranes of sensitive cells.

1. Introduction

Bacteria evolve quickly to counter new antibiotics and treatments for infections [1,2]. Therefore, there is an urgent need for new antibiotics and strategies to combat them, particularly those showing multidrug resistance. In contrast to conventional antibiotics, antimicrobial peptides do not appear to induce antibiotic resistance [3]. Therefore, these peptides raise much interest as potential candidates to develop alternative/adjunct therapeutic strategies [4].

Microcins are a miscellaneous group of low-molecular weight peptides with antibiotic activity, produced by a number of Enterobacteriaceae species, mostly *Escherichia coli* strains [5]. Although most of the microcins inhibit enzymatic pathways, membrane interaction was also postulated to be part of their mechanism of action. Microcin J25 is a plasmid-encoded 21 amino acid antibiotic peptide produced by *E. coli* [6,7] and active against *E. coli*, *Salmonella* and *Shigella* strains [6,8]. The sequence is rich in hydrophobic residues and the backbone is folded in an unusual lasso distinctive structure (Fig. S1) [9–11]. The lasso structure contains a lactam linkage between the α-amino group of Gly1 and the γ-carboxyl of Glu8, forming an eight-residue ring (Gly1–Glu8), which is termed a lariat ring. The 'tail' (Tyr9–Gly21) passes through the ring, with Phe19 and Tyr20 straddling each side of the 'tail', sterically trapping it within the ring [5,9–14].

Microcin J25 exerts antimicrobial activity by means of a dual mechanism of action [7,15,16]: the peptide inhibits transcriptional activity by obstructing the RNA polymerase secondary channel [13,17,18] and affects, independently, the cytoplasmic membrane of *E. coli* and *Salmonella enterica* serovars [15,16,19–22]. In this regard, it was shown that microcin J25 causes dissipation of the electrochemical membrane potential of *S. enterica* and inhibition of respiratory chain enzymes such as NADH, succinate and lactate dehydrogenase, decreasing oxygen consumption rates [16]. The fact that microcin J25 is a membrane-active peptide was also supported by studies carried out on model systems, such as liposomes and Langmuir monolayers [23–25].

Biological membranes are formed by a complex mixture of phosphoglycerides and proteins with a heterogeneous structure at the lateral plane also [26–29]. The cytoplasmic membrane of Gram-negative bacteria is distinctly composed by phosphatidylethanolamine, phosphatidylglycerol and cardiolipine in *ca.* 80:16:4 proportion [27] and lacks phosphatidylcholine, one of the main phospholipids in eukaryotic cells. Therefore, a specific model membrane system for studying biochemical process at molecular level in bacteria is needed.

In this regard, lipid monolayers permit the study of membrane interaction of different molecules by measuring changes in the interfacial tension whilst keeping molecular density, lateral

* Corresponding author. Tel.: +54 381 4248921; fax: +54 381 4248921.
E-mail address: fdupuy@fbqf.unt.edu.ar (F.G. Dupuy).

http://dx.doi.org/10.1016/j.colsurfb.2015.03.048
0927-7765/

packing and phase behavior controlled [30–32]. Lipid bilayer systems, on the other hand, permit a closer approach to the actual accommodation of molecules in biological membranes and can be studied by a wide range of techniques, like infrared spectroscopy, allowing the study of configurational isomerization and lateral packing of hydrocarbon chains and hydration level of membrane interfacial region [33–35].

In the present work, the effect of microcin J25 adsorption on monolayers and bilayers model systems formed by the phospholipids 1,2-dimirystoyl-*sn*-glycero-3-phosphoethanolamine (DMPE), 1,2-dipalmitoyl-*sn*-glycero-3-phospho-rac-(1-glycerol) (DPPG) and the bacterial-like mixture composed DMPE:DPPG 7:3 molar ratio was studied. On one hand, surface pressure at different surface molecular density and peptide concentration in subphase was measured by means of Langmuir monolayers technique. Furthermore, surface morphology was imaged by Brewster angle microscopy (BAM). In addition, infrared spectroscopy (FTIR) experiments in liposomes were carried out. Results from both monolayer and bilayer experiments indicate a preferred interaction of microcin J25 with the bacterial membrane model mixture and a stabilization of ordered states of phospholipids.

2. Materials and methods

2.1. Materials

Chemical reagents, deuterium oxide and culture media were analytical grade from Sigma (St. Louis, USA) whereas solvents HPLC grade were from Merck (Darmstadt, Germany). Dimiristoylphosphatidylethanolamine (DMPE) and dipalmitoylphosphatidylglycerol (DPPG) were purchased from Avanti Polar Lipids (Alabaster, AL, USA) and used without further purification.

2.2. Peptide purification

Microcin J25 was obtained from the supernatant of *E. coli* K-12 MC4100 (*F-araD 139 (argF-lac)205 λ-flbB5301 ptsF25 relA1 prsL150 deoC1*) harboring pTUC203, a low-copy-number recombinant plasmid with the microcin J25 operon cloned [36]. Cells were grown in M9 minimal media (Sigma, St. Louis), supplemented with 0.2% glucose, 1 mM $MgSO_4$ and 1 μg mL^{-1} thiamine. Microcin J25 was purified according to the procedure previously reported [25]. The purity of the microcin preparation was 97%, which appeared homogeneous in two different systems of analytical RP-HPLC (Gilson, Middleton, USA). Concentrations of peptide solutions in methanol were determined by absorbance at 278 nm (ε_{278} = 3340 M^{-1} cm^{-1}).

2.3. Monolayer experiments

Monolayer experiments were carried out in a KSV MiniTrough Langmuir balance (KSV Instruments, KSVNIMA, Biolin Scientific, Sweden), equipped with Teflon trough (70 mm × 240 mm × 8 mm) and two hydrophilic Delrin barriers, for symmetric compression experiments and in a custom-made device equipped with 60 mm × 20 mm × 10 mm Teflon trough and magnetic stirring, for constant area experiments. Surface pressure was measured with a microbalance and Wilhelmy platinum plates (perimeter 2.1 cm). The devices were enclosed in acrylic boxes, and temperature was kept constant at 24 °C. All solvents used for cleaning the trough and the barriers were of analytical grade. Monolayers were formed by spreading 50 nmol of lipid molecules from calibrated chloroform solutions (concentration around 1 mg mL^{-1}) of DMPE, DPPG and DMPE:DPPG (7:3) by means of microsyringes (Hamilton Co., USA). After an equilibration time of 5 min, films were compressed at a rate of 5×10^{-2} nm^2 min^{-1} mol^{-1}. Each compression isotherm was performed at least three times. The standard error was $\pm 5 \times 10^{-3}$ nm^2 for area and ±0.2 mN m^{-1} for surface pressure measurements. Unbuffered 145 mM NaCl was used as subphase (pH *ca.* 6).

Monolayer phase transitions were calculated according to second and third derivatives method of surface pressure-area isotherms [37], whereas surface elasticity was studied calculating the surface compressional modulus [32,38]:

$$C_S^{-1} = A \cdot \frac{\partial \pi}{\partial A}$$

where A and π are mean molecular area and surface pressure, respectively. The thermodynamic parameters of mixing, ΔG_{mix} and ΔH_{mix} were calculated according to [32,39]:

$$\Delta G_{mix} \int_1^5 (A_{PE:PG/MccJ25} - (X_{PE:PG} \cdot A_{PE:PG} + X_{MccJ25} \cdot A_{MccJ25})) \cdot d\pi$$

$$\Delta H_{mix} = \frac{\Delta G_{mix}}{(X_1 \cdot X_2^2 + X_2 \cdot X_1^2) \cdot Z}$$

where A and X are mean molecular area and mole fraction of the corresponding component and Z is the packing fraction parameter [40].

2.4. Peptides adsorption at constant area

DPPG, DMPE and DMPE:DPPG (7:3) solutions were drop-wise spread at the air–water interface using a Hamilton syringe in order to obtain a defined initial surface pressure, π_{init}. After 5 min of equilibration, small aliquots of stock peptide solution (250 μM) was injected into the subphase beneath the phospholipid film in order to obtain a final concentration of peptide in the subphase of 5 μM and the variation of the surface pressure was recorded as a function of time with a constant temperature of 24 °C.

2.5. Brewster angle microscopy

Morphological characteristics of the spread monolayers at air/liquid interface were directly examined by means of Brewster angle microscopy (BAM, Nanofilm EP3sw imaging ellipsometer, Accurion, Göettingen, Germany), equipped with 532 nm laser and 10× objective. A KSV MiniTrough device for monolayer experiments was used and reflectivity of the p-polarized incident laser was measured after the calibration of the actual Brewster angle of the clean subphase (53.1°). Images were visualized with a CCD camera at a resolution of 2 μm. The public software ImageJ (1.43u Wyane Rasband, National of Health, Bethesda, MD) was used for gray level determination in the images recorded during the adsorption process.

2.6. Bilayer experiments

Large unilamellar vesicles of DMPE:DPPG 7:3, DMPE and DPPG were obtained by the extrusion technique (Lipex Biomembranes Inc., Vancouver, Canada) using 100 nm polycarbonate membranes (Poretics, CA, USA). Chloroformic lipid solutions were evaporated under nitrogen stream, followed by 30 min in high vacuum in order to ensure a complete solvent removal. The lipid films were dispersed in deuterated Hepes buffer (10 mM HEPES, 80 mM NaCl, pD = 7.6) by vigorous vortexing at temperatures above the transition one (60 °C) and extruded 10 times with pressurized dry Nitrogen. The final lipid concentration used was 30 mM and was determined measuring total phosphate with the method of Ames [41] after vesicles extrusion.

Infrared spectra were measured in a Nicolet 5700 spectrophotometer (Nicolet™, Thermo-Scientific, MA, USA) equipped with DTGS detector and a purged optic-bench by means of constant flow

of dry air provided by a Parker Balston dry-air generator (model 75-52, Parker Hannifin). Spectra were collected at a resolution of 2 cm^{-1} and each one is the result of 16 averaged measurements.

Microcin J25 at 0.8 mM final concentration was co-incubated with pre-formed liposomes and 20 μL aliquots were placed in a demountable liquid cell equipped with CaF_2 windows and 56 μm Teflon spacers (Harrick Scientific, NY, USA). The temperature of the cell was controlled by a custom-made Peltier device that permits the adjustment of the rate of the temperature scans.

3. Results

3.1. Microcin J25 favorably interacts with lipid monolayers

Previous studies in monolayers determined a low surface activity of microcin J25, in spite of its high hydrophobic character (Fig. S1). Compression isotherms indicated a collapse surface pressure of 5 mN m^{-1} (Fig. S2), whereas Gibbs isotherms experiments showed a maximal surface pressure at equilibrium of 8 mN m^{-1} at peptide concentration in subphase higher than 10 μM [23]. On the other hand, interaction of microcin J25 with membranes has been studied in zwitterionic phosphatidylcholine monolayer model systems [23] and in a higher variety of lipids in bilayer model systems, which showed selective interaction of the peptide with gel phase membranes [16,24,25]. Hence, in order to deepen the mechanism of antimicrobial action of microcin J25, we first studied the peptide adsorption to different bacterial lipids in monolayers.

Consequently, monolayers of DPPG, DMPE and the mixture DMPE:DPPG (7:3) were spread at defined initial surface pressure (π_{init}) and small aliquots of a concentrated peptide solution were injected beneath the monolayer in order to obtain a final microcin J25 concentration of 5 μM in the subphase, while the variation of surface pressure ($\Delta\pi$) was recorded. Peptide adsorption produced an abrupt increase in π in DMPE:DPPG 7:3 monolayers, reaching surface pressure equilibrium values, after around 5 min, higher than microcin J25 adsorption at clean air/water interfaces (Fig. 1A, Inset). At π_{init} below the transition surface pressure (*ca.* 6.8 mN m^{-1}), and independently of phospholipid composition, peptide addition produced an increase of surface pressure. However, around 10 mN m^{-1}, close to liquid-expanded (LE)–liquid-condensed (LC) monolayer phase transition, change in $\Delta\pi$ was null. At surface pressures higher than 10 mN m^{-1}, microcin J25 was able to insert in DPPG and DMPE:DPPG but not in DMPE monolayers (Fig. 1A). The above results show that the antimicrobial peptide interacted more favorably with bacterial-like mixed films and with anionic DPPG monolayers than with DMPE. As a consequence microcin J25 resulted stabilized at the interface and reached surface pressure values higher than the peptide alone.

Favorable microcin J25-membrane interaction was also observed at very low peptide concentration at subphase. Fig. 1B shows that at concentrations below 0.1 μM no increment in surface pressure occurred, whereas in presence of DMPE:DPPG 7:3 mixed monolayer standing at 3 mN m^{-1}, significant surface pressure increments were observed even at the lowest peptide concentration at subphase assayed (*ca.* 7 nM).

3.2. Microcin J25 stabilizes gel phase of bacterial membrane model systems

Compression isotherms of DMPE:DPPG mixture showed a single monolayer phase transition from LE to LC at 7.1 mN m^{-1} with a LE/LC coexistence region with low slope, indicating a good miscibility of the lipid components (Fig. 2A, open circles and Fig. S2). As microcin J25 presented both bactericidal and interfacial activity at nanomolar concentrations, we studied the effects on phospholipid

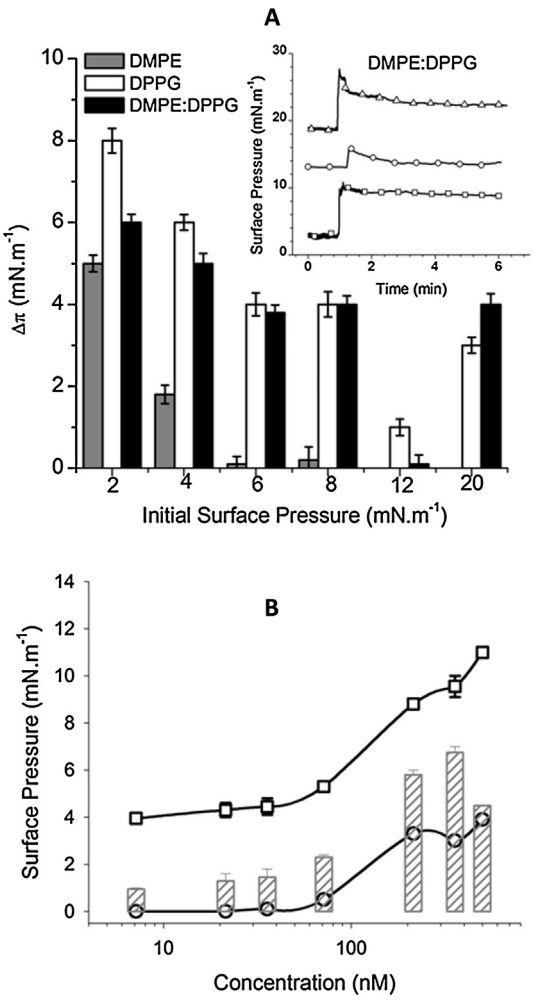

Fig. 1. Microcin J25 adsorption to pre-formed lipid monolayers. (A) DMPE, DPPG and the mixture DMPE:DPPG 7:3 monolayers were spread as monolayers at different surface pressures and a peptide final concentration of 5 μM was injected in 145 mM NaCl subphase. Inset: experimental recording of the surface pressure values of microcin J25 adsorption in DMPE:DPPG 7:3 monolayers. (B) Dependence of microcin J25 subphase concentration on the final surface pressure after peptide adsorption on clean air/water interface (circles) and DMPE:DPPG 7:3 monolayers at 3 mN m^{-1} (squares). Gray bars show net surface pressure increment on lipid monolayers. Data shown are the mean ± SD of three independent experiments.

monolayers of this low amount of microcin J25 in the subphase. DMPE:DPPG monolayers were slowly compressed up to 2 mN m^{-1}, and after letting stand for 5 min, microcin J25 at a final concentration of 16 nM was injected in the subphase, in the absence of stirring in order to avoid disturbances during BAM pictures acquisition. A surface pressure increase of 5 mN m^{-1} was observed, even though at the same subphase concentration microcin J25 produced null $\Delta\pi$ in clean air–water interfaces (Fig. 1B), as discussed above. The monolayer was allowed to stabilize for a further 5 min before the compression was resumed. A cooperative phase transition could still be observed for the microcin J25/DMPE:DPPG mixture at the interface (Fig. 2A, closed circles), as indicated by the flat phase transition region in the area-pressure isotherms. Further compression lead to a steeply increase in surface pressure at the LC state of the isotherm. The surface elasticity of LC monolayer phase of DMPE:DPPG showed no significant differences upon microcin J25 adsorption when compared with control lipid monolayers: the calculated surface compressional modulus of DMPE:DPPG 7:3 at 20 mN m^{-1} in the absence of microcin J25 was 115 ± 15 mN m^{-1} (Fig. S2), whereas for the same lipid mixture after peptide adsorption was of 126 ± 20 mN m^{-1}.

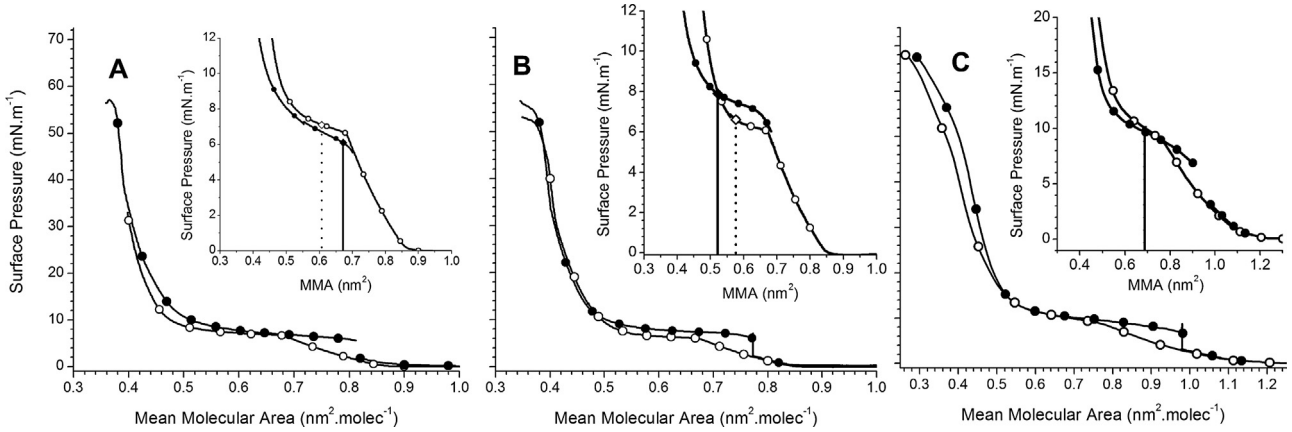

Fig. 2. Monolayer compression isotherms after microcin J25 adsorption. Compression isotherms in the absence (open circles) and in the presence (closed circles) of microcin J25 are shown for lipid monolayers formed by DMPE:DPPG 7:3 (A), DMPE (B) and DPPG (C). The peptide was injected beneath the lipid monolayers previously compressed up to 2 mN m^{-1}. The dotted lines in the insets indicate the formation of condensed domains when peptide free-monolayers were compressed; whereas full lines indicates domain formation when monolayers were compressed after microcin J25 adsoprtion.

However, when microcin J25 was injected in the subphase at nanomolar concentrations, the surface pressure onset of LE–LC phase transition was lowered from 7.1 to 6.1 mN m^{-1}, indicating that the peptide facilitated the pressure-driven transition to liquid-condensed state (Fig. 2A, closed circles). In addition, when molecular area of monolayer was recalculated after microcin J25 injection, taking into account the increased number of molecules present in the interface as a result of peptide adsorption, the phase transition occurred at similar molecular area than in the absence of microcin J25 injection but at a lower surface pressure (Fig. 2A, Inset, closed circles).

On the other hand, when the same experiment was carried out in pure DMPE monolayers, although the antimicrobial peptide induced a significant increase in $\Delta\pi$ when compared to clean air/water interface (Fig. 2B, closed circles), the transition surface pressure of the monolayer measured after microcin J25 injection was higher than control compression isotherms of DMPE in the absence of microcin J25 (Fig. 2B, Inset). In addition, transition surface pressure of DPPG monolayers remained also unchanged when peptide was injected in subphase of lipid films at 3 mN m^{-1} (Fig. 2C).

Thus, a preferential stabilization of the condensed phase in the DMPE:DPPG mixtures induced by microcin J25 could be inferred from surface pressure measurements. In order to confirm this, we used Brewster angle microscopy, which permits to record probe-free images during compression isotherms of monolayers. Fig. 3 shows BAM pictures of DMPE:DPPG mixtures obtained at indicated surface pressures in the absence (A–C) and in the presence (D–F) of microcin J25 injected into the subphase at a π_{init} of 2 mN m^{-1}.

Compression isotherms of lipid mixtures were characterized by a dark homogeneous appearance at surface pressures below 7.1 mN m^{-1} at which LE–LC transition occurs (Fig. 3A). At the monolayer phase transition, bright flower-shaped domains of mixed condensed phase appeared at mean molecular area of 0.61 nm^2 mol^{-1} during compression (Fig. 3B). Finally, condensed phase at surface pressures above 15 mN m^{-1} displayed again homogeneous but, in this case, bright surface (Fig. 3C). Monolayers of pure microcin J25 showed homogeneous surface until peptide monolayer collapse (not shown) and with reflectivity levels higher than films of DMPE:DPPG 7:3 mixture at the same surface pressures (Table 1).

In addition, when microcin J25 was injected into subphase beneath a DMPE:DPPG 7:3 monolayer standing at 2 mN m^{-1}, numerous bright nuclei of condensed phase appeared immediately after peptide injection. Then, upon film compression, higher amounts of condensed domains could be observed in the presence (Fig. 3D and E) than in the absence (Fig. 3A and B) of microcin J25, at the same surface pressure. Domains formed during compression of monolayers in the presence of the antimicrobial peptide were smaller and more rounded in shape and were formed at lower surface pressure when compared with control pure lipid experiments (see Fig. 3A and D). Also, measured reflectivity of condensed domains formed in presence of microcin J25 was higher than reflectivity of control monolayers (Table 1), indicating a close association of the peptide and lipids even at the condensed state.

On the contrary, when microcin J25 was injected in the subphase of DMPE monolayers at 2 mN m^{-1}, lipid condensed domains

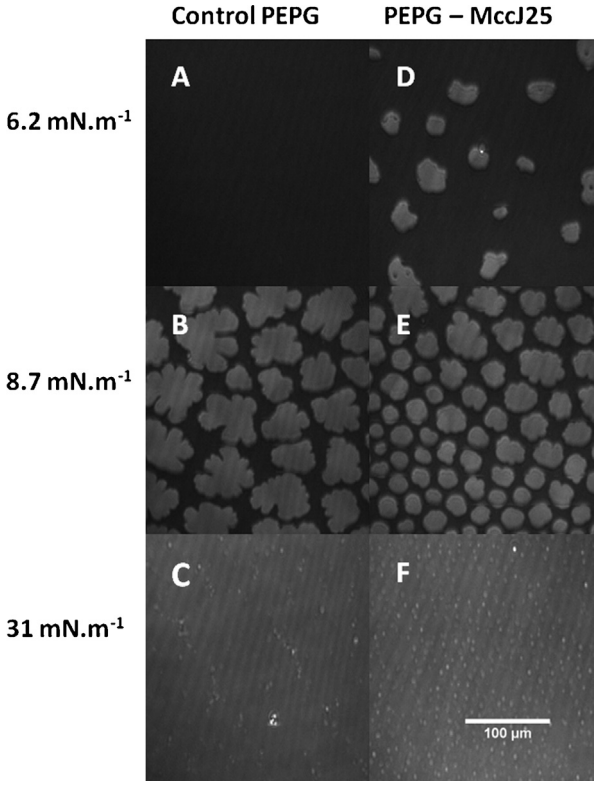

Fig. 3. Influence of microcin J25 on the surface topography of DMPE:DPPG monolayers. Pictures of the control lipid mixture DMPE:DPPG 7:3 (A–C) and of microcin J25/DMP:DPPG after peptide inyection (D–F) where obtained during film compression at a surface pressure of 6.2 (A, D), 8.7 (B, E) and 31 mN m^{-1} (C, F).

Table 1
Reflectivity levels of p-polarized light of Langmuir monolayers formed by the bacterial membrane-like lipid mixture (DMPE:DPPG 7:3), the antimicrobial peptide microcin J25 and after peptide adsorption.

	Reflectivity (R_p) × 10^8 at			
	2 mN m^{-1}	5 mN m^{-1}	10 mN m^{-1}	26 mN m^{-1}
DMPE:DPPG 7:3	26.2 ± 0.9	30.7 ± 0.7	168.8 ± 1.4	173.5 ± 1.2
DMPE:DPPG/microcin J25	26.9 ± 1.1	N.A.	229.8 ± 0.8	367.1 ± 1.6
Microcin J25	68.6 ± 1.8	108.2 ± 2.0	–	–

Results are the mean ± standard error of three independent experiments.

appeared at higher surface pressures when compared to peptide-free control experiments, in agreement with the increase in the LE–LC transition surface pressure of DMPE monolayers observed in the presence of microcin J25. The above results indicate no stabilization of DMPE condensed phase occurred. Similarly, when DPPG monolayers were compresed either in the absence or in the presence of microcin J25 injection in the subphase, condensed domains formed during at the same surface pressure (data not shown).

Thus, condensed phase stabilization induced by microcin J25 could be observed only in DMPE:DPPG mixed monolayers. This could be quantified by analyzing the compression work necessary to form domains of condensed phase in DMPE:DPPG monolayers after microcin J25 adsorption. Taking into account the area under the compression isotherms up to the domains nucleating point (Figs. 2A and 3D, straight lines), the calculated compression work was reduced 40%, from 0.64 to 0.36 kJ mol^{-1}, in the absence and in the presence of microcin J25, respectively, because of the values of molecular area and surface pressure (0.67 nm^2 and 6.1 mN m^{-1} *vs* 0.61 nm^2 and 7.1 mN m^{-1}), at which condensed domains appeared, in presence and in absence of microcin J25, respectively (Fig. 2).

Also, a negative value of −0.24 kJ mol^{-1} for the free energy of mixing was obtained, which agreed with the spontaneous adsorption process of microcin J25 in bacterial-like lipid mixtures. The integer of the isotherm was carried between 1 and 5 mN m^{-1}, in order to avoid the peptide monolayer collapsed state. The negative free energy of mixing also indicated favorable interactions between lipids and microcin J25 molecules in the mixture; actually, the calculated mixing enthalpy was also negative, equal to −0.49 kJ mol^{-1}, which confirmed that molecules interacted more favorably in the mixture than in the pure state.

3.3. *Microcin J25 increases the temperature of gel–liquid crystalline phase transition in DMPE:DPPG liposomes*

Since monolayer experiments indicated favorable interaction of microcin J25 with bacterial membrane model systems and stabilization of the condensed phase, we decided to study the effects of the peptide in bilayer model system by means of FTIR, which is also a probe-free technique. The different absorbance bands of the phospholipids were evaluated in the absence and in the presence of microcin J25 in order to assess if some region of the membrane resulted affected upon peptide binding.

Fig. 4 shows that in bilayers, the components of the DMPE:DPPG 7:3 were mixed and presented a single cooperative gel–liquid crystalline transition at 45 °C. When DMPE:DPPG 7:3 liposomes were incubated with microcin J25, only minor changes in the frequencies of mass center of different bands occurred, suggesting that PE:PG bilayers presented no major structural/conformational changes upon peptide interaction, both in the gel and in the liquid crystalline phase (Fig. 4).

However, the gel to liquid-crystalline phase transition of DMPE:DPPG in the presence of microcin J25 was observed at 5 °C above than that of the control membranes in the absence of the peptide. As revealed by the temperature dependence of the frequency shifts of either symmetric stretching mode of methylenes (Fig. 4A), the scissoring deformation of methylenes (Fig. 4B) and the stretching of carbonyls groups (Fig. 4C) a stabilization of the gel phase upon microcin J25-bilayer interaction was observed, in accordance with the results obtained in monolayers.

Moreover, when DMPE liposomes were heated in the presence of microcin J25, the gel to liquid crystalline transition occurred at the same temperature than in the absence of the peptide (Fig. 4D). Nevertheless, the wavenumber of the methylene-symmetric stretching mode showed decreased values, indicating an ordering of the hydrocarbon chains in the liquid crystalline phase. In the case of pure DPPG vesicles, a slight increment of the gel to liquid crystalline phase transition of less than 2 °C was observed, whereas the wavenumbers of the hydrocarbon chains below and above the transition temperature remained unchanged upon microcin J25 interaction (Fig. 4E). Thus, the gel phase stabilization induced by the antimicrobial peptide microcin J25 occurred mainly in the bacterial like membrane model systems composed by DMPE:DPPG 7:3 in comparison with the pure systems formed by DMPE or DPPG only.

Tridimentional structure of microcin J25 is a surprisingly stable threaded knot folding. Analysis of the Amide I' vibrational mode of the peptide, which senses secondary structrure [42,43], revealed no major changes upon membrane interaction (Fig. S3). The overall Amide I' band of microcin J25 presents maximal intensity at 1649 cm^{-1} and a strong shoulder at 1629 cm^{-1}, which can be assigned to flexible regions of the lasso backbone [9] and distorted β-structures formed by residues in the ring and threaded lasso region of the peptide, respectively [9,10]. The positions of the component bands remained unchanged in the presence of gel phase liposomes, whereas the width of the overall band decreased but only from 60 to 50 cm^{-1} (Fig. S3). In the presence of liquid-crystalline vesicles, no change in the Amide I' band was observed. The absence of major secondary structure rearrangements is expectable for the tight folding of microcin J25 and indicates that peptide–membrane mixing must be enthalpically driven by the interaction of lipids molecules and this hydrophobic antimicrobial peptide.

4. Discussion

The biological activity of microcin J25 ranges from the antimicrobial action against Gram negative bacteria [6,8,16], the anti-mitochondrial effects [44,45] and apoptosis of COS-7 cells [45]. Also, the minimal inhibitory concentration necessary for bactericidal activity varies from 10 nM in sensitive *Salmonella* strains [16,46] to the micromolar range in *E. coli* laboratory strains [6,8,15], clinical isolates and also *Salmonella* strains [46]. Thus, a multi-target mechanism of action seems to be involved in microcin biology, in which peptide–membrane interaction must be taken into account. In this regard, the most sensitive strains showed membrane dysfunction, like inhibition of the respiratory chain, proton motive force dissipation and superoxide production [15,16,20].

However, studies of microcin J25-membrane interaction in bacterial like model systems are still scarce. The present work showed a measurable preferential affinity of microcin J25 toward

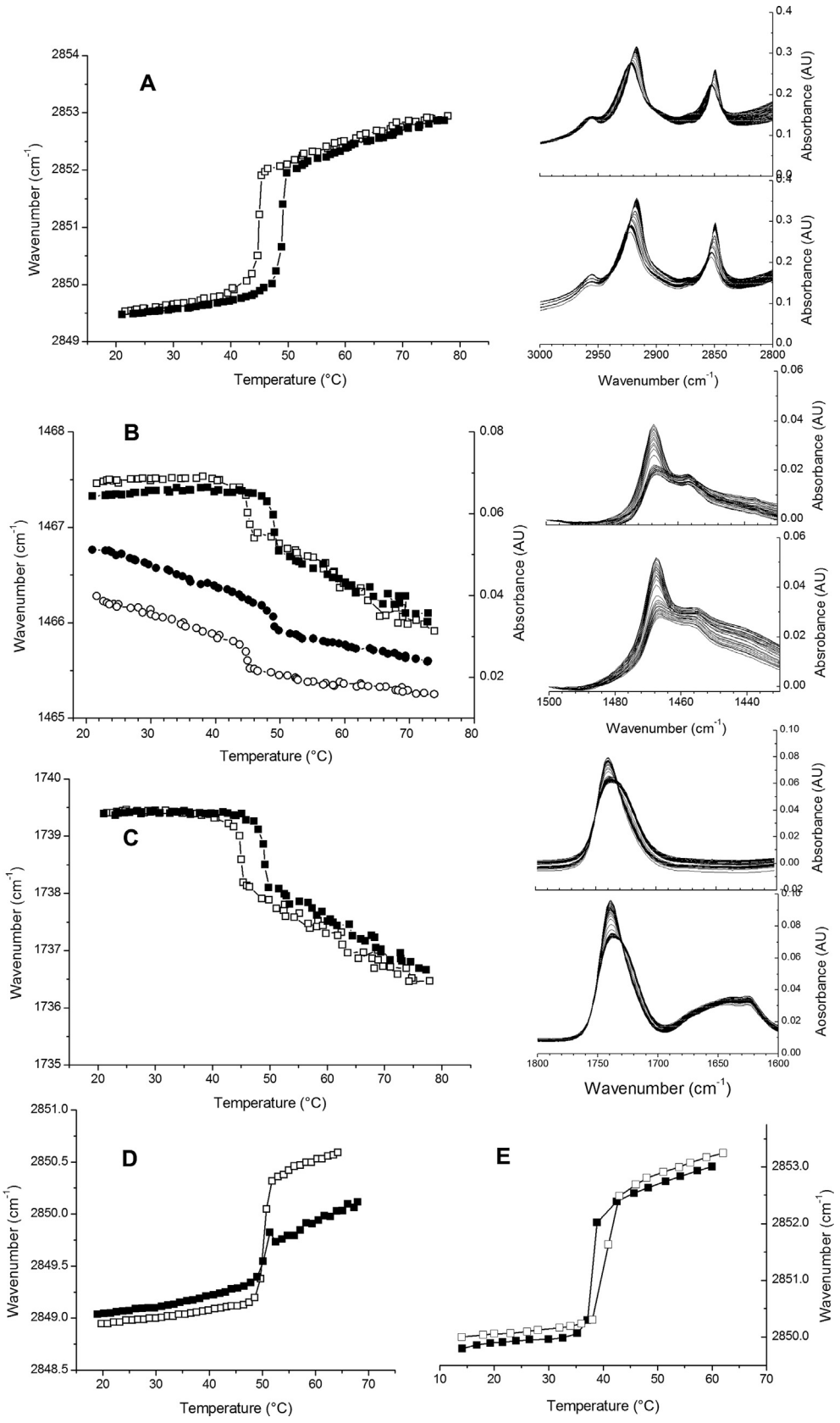

Fig. 4. Membrane perturbation produced by microcin J25 studied by FTIR. The center of mass (left column) of different bands (right column) corresponding to the lipid vibrational modes methylene antisymmetric stretching (A), methylene scissoring (B) and carbonyl stretching (C) of DMPE:DPPG 7:3 liposomes were calculated at different temperatures in the absence (open symbols) and in the presence (closed symbols) of microcin J25. The center of mass of the methylene stretching mode of liposomes formed by DMPE (D) and DPPG (E) in the absence (open symbols) and in the presence (closed symbols) of microcin J25 were calculated at different temperatures.

bacterial membrane model systems, as indicated by the adsorption and the increase in surface pressure on DMPE:DPPG monolayers at nanomolar peptide concentrations in the subphase, *i.e.* not only at the biologically active range but also at concentrations at which microcin J25 was not able to reduce the interfacial tension of clean air–water interface. The higher surface pressure that the antimicrobial peptide was able to reach in presence of lipid monolayers when compared to clean air/water interfaces confirmed the interfacial stabilization of microcin J25 as a consequence of favorable interactions with bacterial-like lipids. Microcin J25 also induced a subtle isothermal decrease on the surface pressure of the LE to LC monolayer phase transition in the DMPE:DPPG 7:3 phospholipid mixture, which was confirmed by imaging monolayers by means of BAM: condensed domains were formed at lower surface pressure in the presence rather than in the absence of microcin J25. Additionally, the increased reflectivity of the films, which depends on the optical thickness and refractive index of the interface [47], after microcin J25 adsorption confirms a close association of the peptide with the lipid films. The decreased size of domains formed during compression in the presence of microcin J25 indicates that the peptide induced either an increase of line tension or a decrease of dipolar repulsion between the condensed domains and the surrounding expanded phase [48].

In agreement with monolayer experiments, when liposomes of DMPE:DPPG 7:3 mixture were co-incubated with microcin J25, an increased melting temperature for the isobaric gel to liquid crystalline phase transition was obtained. Thus, both monolayer and bilayer model systems indicate that ordered phases in bacterial membranes are favored by microcin J25. Ordered phase stabilization explains the cooperative binding isotherms of microcin J25 in gel-phase phosphatidylcholine liposomes [24] and the preference of the peptide toward gel and not liquid-crystalline bilayers. The relevance of these results relies not only on that they were obtained from different techniques but also because experiments were not performed by co-dissolving lipid and peptide before monolayer spreading nor liposome preparation, but by letting microcin J25 to interact with the pre-formed model membranes from the "outside", getting in this way a better mimicking of a physiological scenario.

The effect of lipid condensed phase stabilization upon microcin J25-membrane interaction was observed only in the mixed membrane model systems DMPE:DPPG 7:3. When membrane interaction of microcin J25 was evaluated with pure DMPE or DPPG either in monolayer or bilayer model systems, no preferential stabilization of membrane ordered states could be measured. Although microcin J25 is able to interact with a variety of lipid membranes showing, for example, selective binding to gel phase phosphatidylcholine bilayers [24,25], the differential effects that the peptide exerts in bacterial-like membrane models must be related to its biological effects on membranes of sensitive cells.

In this regard, the bacterial lipids PE and PG present several opposite physicochemical characteristics: the former posses a zwitterionic small head group able to form a hydrogen bond network with similar neighbor lipids [49–51] which lead to stiffer interfaces with lower lateral diffusion rates [52] when compared to membranes formed by PG. The polar head group of the latter lipid is negatively charged, which allows a higher level of hydration at interfacial region when compared to PE [53]. Thus, global properties of the bacterial lipid bilayer must be the result of the counterbalanced contribution to structural integrity, hydration level and surface electrostatics of these dissimilar lipid components.

Gram negative bacteria have an extra outer membranes formed by a asymmetric PE/lipopolysaccharide (LPS) bilayer [54]. The latter is complex lipid molecule, with six or seven fatty acids, usually saturated and bonded to a diglucosamine core, which constitute the lipid A region of the molecule that is linked to the O-antigen by the KDO core [54]. Despite its complex structure, the order parameter of the hydrophobic region of outer membranes is high [55], similar to gel phases. Accordingly, microcin J25 would be able to interact with LPS, owing to its preference to gel phase membranes. However, previous studies have indicated that microcin J25 translocates the outer membrane *via* the porin FhuA [56], a siderophore transporter. In addition, the biological effects that have been described for microcin J25-membrane interaction, like proton-motif force dissipation and respiratory chain enzymes inhibition, are related to inner membrane. Consequently, we focused the present work in model systems of the bacterial inner membrane, even though the study of the effects of microcin J25–LPS interaction is in progress.

Indeed, microcin J25 would not be a membrane-lytic peptide, as no major structural changes in cells as well as model membranes have been reported so far [16,24,25,44]. According to our FTIR results, membrane structure is rather preserved upon microcin J25 interaction, even though the gel phase stability was increased. The order parameter of the gel and liquid crystalline phases showed only a minor increase, as slight decrease on the frequencies of the ν_{symm} CH_2 could be measured. This finding is rather opposite to what is expected of other antibiotic pore-forming peptides that generally induce a decrease of the hydrocarbon chain order parameter and an increase in the frequency of the ν_{symm} CH_2 band [57,58]. In addition, the hexagonal chain packing of the DMPE:DPPG deduced from the position of the $\delta_{scissor}$ CH_2 at 1467 cm^{-1} and the absence of crystalline splitting is also preserved when microcin J25 was added to PE:PG liposomes, indicating that is the gel phase which is actually stabilized by the peptide interaction and no crystal-like phase is induced. The band of $\delta_{scissor}$ CH_2 mode simultaneously decreased in intensity and in frequency during acyl chain melting, indicating that this vibrational mode also sensed the Lβ to Lα lipid transition. Lastly, the interfacial region of DMPE:DPPG mixture also sensed the increased temperature of phase transition produced by microcin J25, although the $\nu_{C=O}$ frequencies showed no major changes but a slight increase in the liquid-crystalline, suggesting a dehydration of carbonyl groups in the disordered state of the membrane. Also, surface elasticity in monolayers of DMPE:DPPG 7:3 mixture was not affected by microcin J25. Consequently, the biological effects of microcin J25 on biomembranes would not be a disruption of the bilayer integrity but an alteration of its physicochemical properties as a consequence of gel phase stabilization, such as interface thickening by peptide adsorption and increased ordered/disordered ratio.

Lipid bilayers of biological membranes can present lateral pressure fluctuations as a result of the high compressibility of the phospholipids in disordered states [51,59], especially in the presence of ordered/disordered phase coexistence in complex mixtures like those encountered in cells or induced by protein insertion and conformational changes within the membranes [51]. Thus, adsorption of microcin J25 at low surface pressure, stabilization of gel/condensed phases and the increase in the number of condensed domains like those observed in the present work in membrane model systems could actually take place in the antimicrobial mechanism of action of microcin J25. Membrane defects and perturbation of the bilayer permeability as a consequence of changes in the lipid phases have been postulated being involved in the biological activity of other antibiotic peptides [29,60,61].

In fact, the increase in small solute permeability in sensitive cells and in model membranes [16,24], the dysfunction of the respiratory chain observed in highly sensitive bacteria [25] and the preferential affinity of microcin J25 to ordered membranes [24] can be integrated altogether in a common pathway along with the presents results. The high affinity of microcin J25 to ordered membranes and the increase in the number of condensed domains induce defects in the lateral packing of the lipids, impairing normal diffusion of membrane-embedded components, respiratory chain enzymes

activity and increasing permeability of small solutes, contributing to bactericidal effects in sensitive cells.

5. Conclusions

The membrane activity of the antibiotic peptide microcin J25 was evaluated in bacterial model membranes, both in monolayer and bilayer systems by means of probe-free techniques. The peptide readily interacted with bacterial-like membranes and produced a stabilization of the membrane ordered states and facilitated the formation of condensed domains. This membrane perturbation explains the increased permeability toward small solutes observed in model as well as biological membranes.

Acknowledgements

The authors thank to Secretaría de Ciencia y Técnica de la Universidad Nacional de Tucumán (Grants 26/D228), Agencia Nacional de Promoción Científica y Técnica (grant PICT 2998) and Consejo Nacional de Investigaciones Científicas y Técnicas (grant PIP 2518) for funding. R.D.M and F.G.D are CONICET career researchers. All the authors contributed in the manuscript writing. M.R.R and F.G.D carried out the experiments. We specially thank to Dr. Bruno Maggio, at Centro de Investigaciones en Quimica Biologica de Cordoba CIQUIBIC-CONICET/UNC, for receiving M.R.R in his laboratory for BAM and Langmuir monolayer measurements.

Appendix A. Supplementary data

Supplementary data associated with this article can be found, in the online version, at http://dx.doi.org/10.1016/j.colsurfb.2015.03.048.

References

[1] J.L. Anaya-Lopez, J.E. Lopez-Meza, A. Ochoa-Zarzosa, Crit. Rev. Microbiol. 39 (2012) 180–195.
[2] S.T. Cole, Philos. Trans. R. Soc. Lond. B: Biol. Sci. 369 (2014) 20130430.
[3] P.G. Arnison, M.J. Bibb, G. Bierbaum, A.A. Bowers, T.S. Bugni, G. Bulaj, J.A. Camarero, D.J. Campopiano, G.L. Challis, J. Clardy, P.D. Cotter, D.J. Craik, M. Dawson, E. Dittmann, S. Donadio, P.C. Dorrestein, K.D. Entian, M.A. Fischbach, J.S. Garavelli, U. Goransson, C.W. Gruber, D.H. Haft, T.K. Hemscheidt, C. Hertweck, C. Hill, A.R. Horswill, M. Jaspars, W.L. Kelly, J.P. Klinman, O.P. Kuipers, A.J. Link, W. Liu, M.A. Marahiel, D.A. Mitchell, G.N. Moll, B.S. Moore, R. Muller, S.K. Nair, I.F. Nes, G.E. Norris, B.M. Olivera, H. Onaka, M.L. Patchett, J. Piel, M.J. Reaney, S. Rebuffat, R.P. Ross, H.G. Sahl, E.W. Schmidt, M.E. Selsted, K. Severinov, B. Shen, K. Sivonen, L. Smith, T. Stein, R.D. Sussmuth, J.R. Tagg, G.L. Tang, A.W. Truman, J.C. Vederas, C.T. Walsh, J.D. Walton, S.C. Wenzel, J.M. Willey, W.A. van der Donk, Nat. Prod. Rep. 30 (2013) 108–160.
[4] M.C. Chalón, L. Acuña, R.D. Morero, C.J. Minahk, A. Bellomio, Food Res. Int. 45 (2012) 735–744.
[5] S. Duquesne, D. Destoumieux-Garzon, S. Zirah, C. Goulard, J. Peduzzi, S. Rebuffat, Chem. Biol. 14 (2007) 793–803.
[6] R.A. Salomon, R.N. Farias, J. Bacteriol. 174 (1992) 7428–7435.
[7] P.A. Vincent, R.D. Morero, Curr. Med. Chem. 16 (2009) 538–549.
[8] S. Sable, A.M. Pons, S. Gendron-Gaillard, G. Cottenceau, Appl. Environ. Microbiol. 66 (2000) 4595–4597.
[9] M.J. Bayro, J. Mukhopadhyay, G.V.T. Swapna, J.Y. Huang, L.-C. Ma, E. Sineva, P.E. Dawson, G.T. Montelione, R.H. Ebright, J. Am. Chem. Soc. 125 (2003) 12382–12383.
[10] K.J. Rosengren, R.J. Clark, N.L. Daly, U. Göransson, A. Jones, D.J. Craik, J. Am. Chem. Soc. 125 (2003) 12464–12474.
[11] K.-A. Wilson, M. Kalkum, J. Ottesen, J. Yuzenkova, B.T. Chait, R. Landick, T. Muir, K. Severinov, S.A. Darst, J. Am. Chem. Soc. 125 (2003) 12475–12483.
[12] D.J. Clarke, D. Campopiano, Org. Biomol. Chem. 5 (2007) 2564–2566.
[13] J. Mukhopadhyay, E. Sineva, J. Knight, R.M. Levy, R.H. Ebright, Mol. Cell 14 (2004) 739–751.
[14] K.P. Yan, Y. Li, S. Zirah, C. Goulard, T.A. Knappe, M.A. Marahiel, S. Rebuffat, ChemBioChem 13 (2012) 1046–1052.
[15] A. Bellomio, P.A. Vincent, B.F. de Arcuri, R.N. Farias, R.D. Morero, J. Bacteriol. 189 (2007) 4180–4186.
[16] M.R. Rintoul, B.F. de Arcuri, R.A. Salomon, R.N. Farias, R.D. Morero, FEMS Microbiol. Lett. 204 (2001) 265–270.
[17] K. Adelman, J. Yuzenkova, A.L. Porta, N. Zenkin, J. Lee, J.T. Lis, S. Borukhov, M.D. Wang, K. Severinov, Mol. Cell 14 (2004) 753–762.
[18] M.A. Delgado, M.R. Rintoul, R.N. Farias, R.A. Salomon, J. Bacteriol. 183 (2001) 4543–4550.
[19] A. Bellomio, P.A. Vincent, B.F.d. Arcuri, R.A. Salomón, R.D. Morero, R.N. Farías, Biochem. Biophys. Res. Commun. 325 (2004) 1454–1458.
[20] M.C. Chalón, A. Bellomio, J.O. Solbiati, R.D. Morero, R.N. Farias, P.A. Vincent, FEMS Microbiol. Lett. 300 (2009) 90–96.
[21] F.G. Dupuy, M.V. Chirou, B.F. de Arcuri, C.J. Minahk, R.D. Morero, Biochim. Biophys. Acta 1790 (2009) 1307–1313.
[22] P.A. Vincent, A. Bellomio, B.F. de Arcuri, R.N. Farias, R.D. Morero, Biochem. Biophys. Res. Commun. 331 (2005) 549–551.
[23] A. Bellomio, R.G. Oliveira, B. Maggio, R.D. Morero, J. Colloid Interface Sci. 285 (2005) 118–124.
[24] F. Dupuy, M.L. Fanani, B. Maggio, Langmuir 27 (2011) 3783–3791.
[25] M.R. Rintoul, B.F.d. Arcuri, R.D. Morero, Biochim. Biophys. Acta 1509 (2000) 65–72.
[26] L.A. Bagatolli, J.H. Ipsen, A.C. Simonsen, O.G. Mouritsen, Prog. Lipid Res. 49 (2010) 378–389.
[27] Y. Feng, J.E. Cronan, J. Biol. Chem. 284 (2009) 29526–29535.
[28] S. Mazor, T. Regev, E. Mileykovskaya, W. Margolin, W. Dowhan, I. Fishov, Biochim. Biophys. Acta 1778 (2008) 2505–2511.
[29] R.M. Epand, R.F. Epand, Biochim. Biophys. Acta 1788 (2009) 289–294.
[30] H. Brockman, Curr. Opin. Struct. Biol. 9 (1999) 438–443.
[31] P. Dynarowicz-Latka, A. Dhanabalan, O.N. Oliveira Jr., Adv. Colloid Interface Sci. 91 (2001) 221–293.
[32] G. Gaines, Insoluble Monolayers at Liquid–Gas Interfaces, Interscience Publishers, New York, 1966.
[33] J.L. Arrondo, F.M. Goni, Chem. Phys. Lipids 96 (1998) 53–68.
[34] J.K. Kauppinen, D.J. Moffatt, H.H. Mantsch, D.G. Cameron, Appl. Spectrosc. 35 (1981) 271–276.
[35] R.N. Lewis, R.N. McElhaney, Biochim. Biophys. Acta 1828 (2013) 2347–2358.
[36] J.O. Solbiati, M. Ciaccio, R.N. Farias, R.A. Salomon, J. Bacteriol. 178 (1996) 3661–3663.
[37] H.L. Brockman, C.M. Jones, C.J. Schwebke, J.M. Smaby, D.E. Jarvis, J. Colloid Interface Sci. 78 (1980) 502–512.
[38] J.T. Davies, E.K. Rideal, Interfacial Phenomena, 2nd ed., Academic Press, New York, 1963.
[39] S.R. Dennison, F. Harris, D.A. Phoenix, Langmuir–Blodgett approach to investigate antimicrobial peptide–membrane interactions, in: Advances in Planar Lipid Bilayers and Liposomes, Academic Press, 2014, pp. 83–110 (Chapter 3).
[40] P. Sospedra, M. Espina, M.J. Gomara, M.A. Alsina, I. Haro, C. Mestres, J. Colloid Interface Sci. 244 (2001) 87–96.
[41] B.N. Ames, V.G. Elizabeth, F. Neufeld, Assay of inorganic phosphate, total phosphate and phosphatases, in: Methods in Enzymology, Academic Press, 1966, pp. 115–118.
[42] J.L. Arrondo, A. Muga, J. Castresana, F.M. Goni, Prog. Biophys. Mol. Biol. 59 (1993) 23–56.
[43] M. Jackson, H.H. Mantsch, Crit. Rev. Biochem. Mol. Biol. 30 (1995) 95–120.
[44] M. Niklison Chirou, A. Bellomio, F. Dupuy, B. Arcuri, C. Minahk, R. Morero, FEBS J. 275 (2008) 4088–4096.
[45] M.V. Niklison-Chirou, F. Dupuy, L.B. Pena, S.M. Gallego, M.L. Barreiro-Arcos, C. Avila, C. Torres-Bugeau, B.E. Arcuri, A. Bellomio, C. Minahk, R.D. Morero, Int. J. Biochem. Cell Biol. 42 (2010) 273–281.
[46] P.A. Vincent, M.A. Delgado, R.N. Farias, R.A. Salomon, FEMS Microbiol. Lett. 236 (2004) 103–107.
[47] C. Lheveder, J. Meunier, S. Hénon, Brewster angle microscopy, in: A. Baszkin, W. Norde (Eds.), Physical Chemistry of Biological Interfaces, Marcel Dekker Inc., New York, Basel, 2000, pp. 559–576.
[48] D. Andelman, F. Broçhard, J. Joanny, J. Chem. Phys. 86 (1987) 3673–3681.
[49] J.M. Boggs, Biochim. Biophys. Acta 906 (1987) 353–404.
[50] B. Pozo Navas, K. Lohner, G. Deutsch, E. Sevcsik, K.A. Riske, R. Dimova, P. Garidel, G. Pabst, Biochim. Biophys. Acta 1716 (2005) 40–48.
[51] J.M. Seddon, G. Cevc, R.D. Kaye, D. Marsh, Biochemistry 23 (1984) 2634–2644.
[52] E. Madrid, S.L. Horswell, Langmuir 29 (2013) 1695–1708.
[53] P. Garidel, A. Blume, Eur. Biophys. J. 28 (2000) 629–638.
[54] R.J. Kadner, Cytoplasmic membrane, in: F.C. Neidhardt (Ed.), *Escherichia coli* and *Salmonella*. Cellular and Molecular Biology, American Society of Microbiology, University of Michigan Medical School, Ann Harbor, Michigan, 1996, pp. 58–87.
[55] E.T. Rietschel, T. Kirikae, F.U. Schade, U. Mamat, G. Schmidt, H. Loppnow, A.J. Ulmer, U. Zahringer, U. Seydel, F. Di Padova, et al., FASEB J. 8 (1994) 217–225.
[56] D. Destoumieux-Garzón, S. Duquesne, J. Peduzzi, C. Goulard, M. Desmadril, L. Letellier, S. Rebuffat, P. Boulanger, Biochem. J. 389 (2005) 869–876.
[57] P. Castellano, G. Vignolo, R.N. Farias, J.L. Arrondo, R. Chehin, Appl. Environ. Microbiol. 73 (2007) 415–420.
[58] S.R. Dennison, J. Howe, L.H. Morton, K. Brandenburg, F. Harris, D.A. Phoenix, Biochem. Biophys. Res. Commun. 347 (2006) 1006–1010.
[59] N. Payne, D. Phillips, A. Puri, G. Scherphof, J. Sowinski, Liposomes, a practical approach.
[60] A. Fernandez-Botello, F. Comelles, M.A. Alsina, P. Cea, F. Reig, J. Phys. Chem. B 112 (2008) 13834–13841.
[61] P. Wadhwani, R.F. Epand, N. Heidenreich, J. Burck, A.S. Ulrich, R.M. Epand, Biophys. J. 103 (2012) 265–274.